Jets at all Scales
Proceedings IAU Symposium No. 275, 2011
G. E. Romero, R. A. Sunyaev & T. Belloni, eds.

doi:10.1017/S1743921310016091

Suzaku studies of microquasars

Yoshihiro Ueda and Megumi Shidatsu

Department of Astronomy, Kyoto University,
Kyoto 606-8502, Japan
email: ueda@kusastro.kyoto-u.ac.jp

Abstract. We report our recent results from multiwavelengths studies of microquasars, focusing on X-ray data of GX 339–4 and GRS 1915+105 obtained with *Suzaku* and other observatories. The broad band coverage and high energy resolution achieved with *Suzaku* (or a combination of *Chandra*/HETGS and *RXTE*) enable us to perform the most reliable spectral analysis both on iron-K features and continuum, and thus to best constrain the accretion disk structure of microquasars and its relation to the jet formation at various mass accretion rates.

Keywords. accretion, accretion disks — black hole physics — X-rays: individual (GX 339–4, GRS 1915+105)

1. Suzaku results on GX 339–4 in the low/hard State

1.1. *Introduction*

GX 339–4 is a transient Galactic black hole binary (BHB) discovered in the early 1970s. Though being one of the best studied canonical BHBs, the accretion flow geometry as a function of mass accretion rate is not firmly established, and is still a subject of intensive investigation. In the very high state, Miller *et al.* (2008) reported the detection of an extremely broad iron-K emission line from *Suzaku* spectra implying a rapid spin of the black hole. This was questioned by Yamada *et al.* (2009), however, who showed that the same data are consistent with a non-rotating black hole, rather supporting the earlier result by Makishima *et al.* (1986) in the high/soft state. Miller *et al.* (2006) suggested that the standard disk of GX 339–4 extends to the innermost stable circular orbit (ISCO) in bright phases of the low/hard state, based on the detection of a relativistically broadened iron-K line, whereas the Tomsick *et al.* (2009) result using *Suzaku* data at a fainter flux level indicates that the disk is truncated at a much larger radius than the ISCO.

To reveal the inner disk structure and the origin of the continuum emission in the low/hard state, we observed GX 339–4 using the X-ray satellite *Suzaku* in 2009 March, when it became active and stayed in the low/hard state. Quasi-simultaneous near-infrared observations were performed with the *Infrared Survey Facility* (*IRSF*) 1.4 m telescope to reveal the jet activity. We refer the readers to Shidatsu *et al.* (2010) for details.

1.2. *X-Ray Spectra*

With *Suzaku*, we have obtained the best quality simultaneous, broad band X-ray spectra ever obtained from GX 339–4 in the low/hard state, covering the 0.5–310 keV band. The overall continuum in the 2–100 keV band can be roughly approximated by a power law of a photon index of $\approx$1.5, above which a sharp decline consistent with an exponential cutoff is present (see Figure 1, middle panel). This strongly suggests a thermal origin for the continuum, although small contribution from non-thermal components is not completely ruled out. Following the previous studies of BHBs in the low/hard state with *Suzaku*,

we adopt models consisting of emission from a standard accretion disk and its thermal Comptonization by a hot corona. The disk emission is represented by the multi-color disk (MCD) model (Mitsuda *et al.* 1984). For the Comptonization component, we employ the `compPS` model in XSPEC (Poutanen & Svensson 1996), which is able to take into account a reflection component from the disk.

We find that the broad band X-ray spectra is dominated by the thermal Comptonization component with an electron temperature of ≈170 keV. The contribution from the direct disk component is very small, indicating that the inner disk is almost fully covered by the hot corona. The Comptonizing corona has at least two optical depths, $\tau = 0.91$ and 0.25. This implies an inhomogeneous structure in the clouds. Similar results have been obtained from other canonical BHBs in the low/hard state with *Suzaku* (e.g., Makishima *et al.* 2008). The best-fit model and unfolded spectrum is plotted in the top panel of Figure 1.

The analysis of the iron-K line profile yields an inner disk radius of $(15^{+10}_{-7})R_{\rm g}$ ($R_{\rm g}$ represents the gravitational radius GM/c^2, where G, M, and c is the gravitational constant, black hole mass, and light velocity, respectively), with an inclination angle of $i = 52^{+8}_{-5}$ degrees. This radius is consistent with that estimated from the continuum fit by assuming the conservation of the photon number in Comptonization. Our results indicate that the standard disk of GX 339–4 is truncated in the low/hard state. Comparing our $R_{\rm in}$ value with that derived from the 2008 *Suzaku* observation (Tomsick *et al.* 2009), when the 1–100 keV flux is 14 times fainter than in our epoch, we can study how the inner edge of the accretion disk evolves during the low/hard state as a function of luminosity. The XIS spectra, best-fit model, and ratio between the data and continuum model are plotted in Figure 2; it is seen that the iron-K line in the 2008 data is significantly narrower than that observed in 2009. The resulting inner disk radius is found to be $R_{\rm in} = 680^{+740}_{-310}R_{\rm g}$ when we assume an inclination angle of $i = 52^\circ$ and an emissivity index of -2.3 as obtained from our observations. These results suggest that the inner edge significantly moved inward as the luminosity increased from 2008 to 2009 even if the source was commonly observed in the low/hard state.

1.3. *Spectral Energy Distribution (SED)*

We examine the origin of the multiwavelength SED of GX 339–4 in the low/hard state with different emission components, utilizing our quasi-simultaneous near infrared and X-ray spectra combined with previous data (Figure 3). There we plot the estimated contribution of the "intrinsic" MCD component including photons that are Compton-scattered in the corona, through the photon number conservation. The upper limit of the contribution from the companion star is also plotted.

Our *IRSF* spectrum shows a slightly steeper slope (an energy index of $\alpha \approx -0.1$) than the radio one; the corresponding $J - K_{\rm s}$ color is similar to that of the 1981 observations compiled by Corbel & Fender (2002). As shown by them, this color is consistent with a superposition of two different components with $\alpha = -0.6$ and $\alpha = 2.1$, which can be explained by the optically *thin* synchrotron radiation from the jets and the reprocessed, thermal emission from irradiated outer parts of the disk, respectively (see also Markoff *et al.* 2003 and Gandhi *et al.* 2010). It is thus indicated that the transition point from optically thick to thin regime of the synchrotron emission must appear at frequencies just below or around the near-infrared band, $\sim 10^{14}$ Hz. Based on a simple analysis, we estimate the magnetic field and size of the jet base to be $\sim 10^5$ G and $\sim 10^9$ cm, respectively. The synchrotron self Compton component is estimated to be $< 1\%$ of the total X-ray flux.

https://doi.org/10.1017/S1743921310016091 Published online by Cambridge University Press

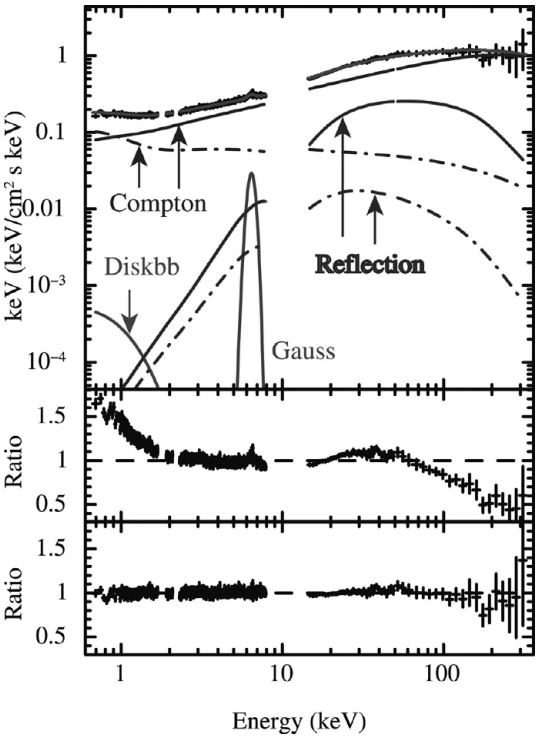

Figure 1. (Top) Unfolded spectrum of GX 339–4 in the low/hard state observed with *Suzaku* in 2009 March. The continuum is described by the double `compPS` + MCD model. The Galactic absorption is corrected. The reflection component for each Comptonized continuum and the iron-K emission line (Gaussian) are separately plotted. (Middle) Spectral ratio between the data and a single power law model fitted to the 2–100 keV range. (Bottom) Spectral ratio between the data and the best-fit model.

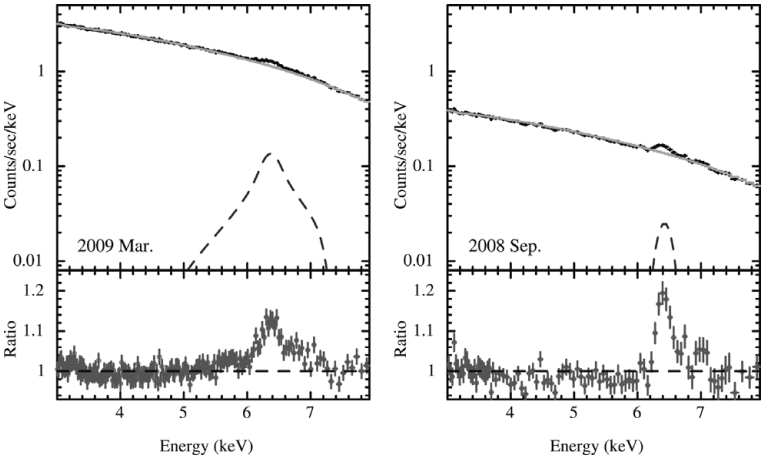

Figure 2. (Upper) *Suzaku* XIS spectra of GX 339–4 in the 3–8 keV band, fitted with the `diskline` model for the iron-K emission line. (Lower) The spectral ratio between the data and the continuum model from which the diskline component is excluded. (Left) The 2009 March data. (Right) The 2008 September data (Tomsick *et al.* 2009).

https://doi.org/10.1017/S1743921310016091 Published online by Cambridge University Press

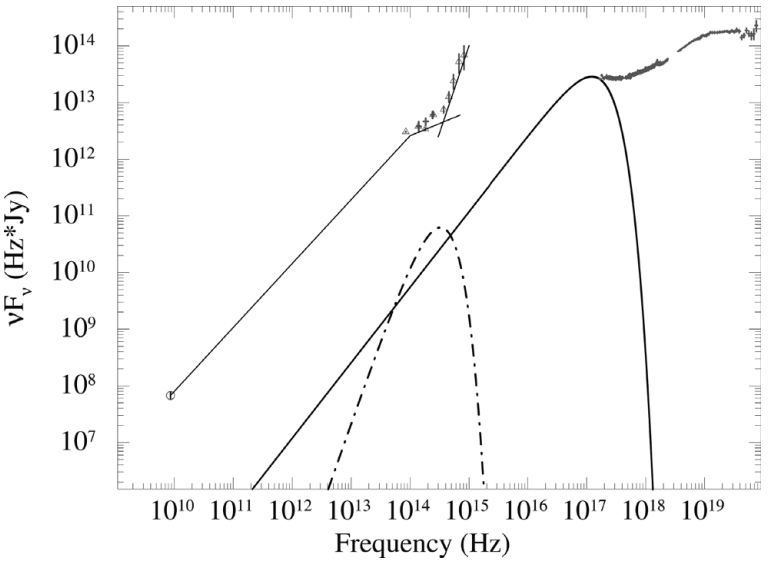

Figure 3. Multiwavelength SED of GX 339–4 in 2009 March, corrected for the interstellar absorption/extinction by assuming $A_V = 3.7$. The radio flux at 8640 MHz is estimated from the empirical relation with the 20–100 keV flux obtained by Corbel *et al.* (2003). In the infrared to optical band, the data from our *IRSF* observations (crosses) are plotted together with those obtained in 1981 compiled by Corbel & Fender (2002) whose flux level is adjusted to fit our K_s-band flux (triangles). The thick solid curve shows an estimated contribution from the intrinsic MCD emission that includes Compton-scattered photons. The dot-dashed curve represents the upper limit of the contribution from the companion star. The broken power law (thin solid lines) corresponds to an estimated contribution from the compact jet, while the steep power law component represents the thermal emission from the irradiated outer disk.

2. Recent Progress in X-ray Studies of GRS 1915+105

2.1. *Introduction*

GRS 1915+105 is the brightest microquasar in our Galaxy, providing us with a unique opportunity to study the accretion flow onto a black hole at high fractions of Eddington ratio (for a review, see Fender & Belloni 2004). Belloni *et al.* (2000) identified 12 "Classes" of the X-ray variability pattern, and found that the instantaneous spectral state of GRS 1915+105 can be divided into three basic states, States A, B, and C, where the source undergoes frequent transition (oscillations) or stays stable. The correspondence between the three states of GRS 1915+105 and canonical states observed in normal black holes (i.e., the low/hard, intermediate or very high, high/soft states) is not completely understood, however.

Here we report our recent results on GRS 1915+105 observed in the stable "soft state" (Class ϕ) with *Chandra*/HETGS and *RXTE*, and in the stable "hard state" (Class χ) and limit-cycle oscillations (Class θ) with *Suzaku*. Instead of standard models usually applied to canonical black hole binaries (e.g., MCD plus a power law), we consider more physically motivated models for the continuum to discuss the nature of the accretion flow. The good energy resolution achieved with *Chandra*/HETGS and *Suzaku*/XIS enable us to examine the disk geometry from the iron-K emission line, as well as the property of the disk wind from the absorption lines. We stress that for correct spectral modelling of GRS 1915+105, accurate interstellar absorptions with non Solar abundances should be taken into account; otherwise, an artificial broad iron-K line feature would easily appear, for instance. Also, one needs to take the effects by the dust-scattering component into

https://doi.org/10.1017/S1743921310016091 Published online by Cambridge University Press

account, in particular for spectral analysis in variable states. For details, we refer the readers to Ueda, Yamaoka, & Remillard (2009) for the stable "soft state" and Ueda *et al.* (2010) for the stable "hard state" and oscillations, respectively.

2.2. *Chandra Observation of GRS 1915+105 in "Soft State"*

Simultaneous *Chandra* HETGS and *RXTE* observations of GRS 1915+105 were performed in its stable "soft state" (or State A) on 2007 August 14. The X-ray flux increased with spectral hardening around the middle of the *Chandra* observation, after which the 67 Hz quasi periodic oscillation (QPO) became significant.

The HETGS spectra reveal at least 32 narrow absorption lines from highly ionized ions, including Ne, Mg, Si, S, Ar, Ca, Cr, Mn, Fe. By fitting to the absorption line profiles by Voigt function, we find that the absorber has outflow velocities of ≈150 and ≈500 km s^{-1} with a line-of-sight velocity dispersion of ≈70 and ≈200 km s^{-1} for the Si XVI and Fe XXVI ions, respectively, indicating that the wind has a non-uniform dynamical structure along the line-of-sight. The location of the absorber is estimated at $\sim 10^5 R_{\rm g}$ from the source, consistent with thermally and/or radiation driven winds. The mass outflow rate carried by the wind is estimated to be $\sim 10^{19}$ g s^{-1} for an assumed solid angle of $\Omega/4\pi = 0.2$. Neilsen & Lee (2009) discuss a possibility that such wind regulates the jet formation.

The continuum spectra obtained with *RXTE* in the 3–25 keV band can be well described with a thermal Comptonization with an electron temperature of ≈4 keV and an optical depth of ≈5 from seed photons from the standard disk extending down to $(4-7)R_{\rm g}$. In this interpretation, most of the radiation energy is produced in the Comptonization corona, which completely covers the inner part of the disk. This is consistent with the absence of a very broad component in the iron-K emission line.

2.3. *Suzaku Observations of GRS 1915+105 in "Hard State" and Oscillations*

Suzaku observed GRS 1915+105 from 2005 October 16 to 18 for a net exposure of ≈80 ks. The light curves are shown in Figure 4. Around the epoch, a large multiwavelength campaign was conducted involving other space and ground observatories (for the preliminary results, see Ueda *et al.* 2006). We made spectral analysis of the *Suzaku* data for four distinct states, "stable" state (State C in Class χ), "oscillation high" state (State C in Class θ), and "oscillation med" and "oscillation low" states (State A in Class θ), sorted by the hard X-ray flux (see Figure 4). The XIS spectra in the 5–9 keV band in these states are plotted in Figure 5. The main results from the *Suzaku* observation are summarized as follows:

(*a*) The *Suzaku* broad band spectra of GRS 1915+105 band both in the stable and oscillation states are commonly represented with a model consisting of a MCD component, its strong Comptonization (modelled by *eqpair*, Coppi 1999), and a reflection component, over which the opacity of the highly ionized disk wind (including iron-K absorption lines and edge) is applied. The Comptonized component dominates the flux above ∼3 keV.

(*b*) The Comptonization is made by optically-thick ($\tau \approx 7$–10), non-thermal / thermal ($T \approx 2$–3 keV) hybrid plasmas. The non-thermal electrons are produced with 10–60% of the total energy input to the plasma with a power law index of ≈3–4, which account for the hard X-ray tail above ∼50 keV.

(*c*) During the limit-cycle oscillation, the reflection component as estimated by the iron-K emission line is the largest during the dip phase but disappears in the flare phase. We interpret this as evidence for self-shielding effects that Comptonized photons are obscured by the surrounding cool region of the expanded disk when viewed at a very high inclination angle from the outer disk. This is illustrated in Figure 6. The evolution

https://doi.org/10.1017/S1743921310016091 Published online by Cambridge University Press

of the inner disk geometry is in accordance with theoretical predictions. The idea also explains the anti-correlation between the soft X-ray and near-IR fluxes reported by Arai *et al.* (2009) on a long time scale (∼days), and by Ueda *et al.* (2006) on a short time scale (∼minutes) during the oscillations.

(*d*) The disk wind, traced by iron-K absorption lines of Fe XXV and Fe XXVI, always exists during the oscillation and its ionization well correlates with the X-ray flux. This supports the photoionization origin. In the stable state, the iron-K absorption lines are not detected probably because it is too highly ionized and/or the scale height is small.

(*e*) The disk parameters suggest that the inner disk structure of GRS 1915+105 is similar to that in the very high state of canonical black hole binaries. The spectral variability in the oscillation state is explained by the change of the disk geometry and of physical parameters of Comptonizing corona, particularly the fractional power supplied to the acceleration of non-thermal particles.

2.4. *Summary*

The unprecedentedly high quality spectra of GRS 1915+105 obtained with *Chandra* and *Suzaku* have revealed the complex accretion disk structure and its evolution during the limit-cycle oscillations for the first time. We suggest that optically thick and low temperature Comptonization process, sometimes dominated that by non-thermal electrons, is a key phenomenon to understand black hole accretion flows at high fractions of Eddington ratio, and hence must be considered in theoretical models. In the near future, *Astro-H* will greatly contribute to this field with the excellent energy resolution and large effective area in the iron-K band.

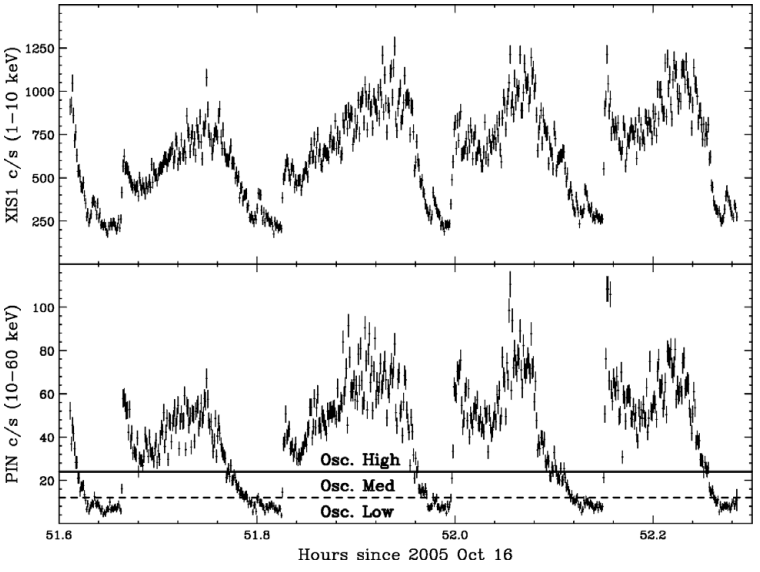

Figure 4. A representative example of *Suzaku* light curves in the 1–10 keV (XIS, upper) and 10–60 keV (PIN, lower) bands during oscillations (Class θ). The bin size is 16 seconds. The horizontal lines in the lower panel correspond to the thresholds between oscillation high/med and med/low states.

https://doi.org/10.1017/S1743921310016091 Published online by Cambridge University Press

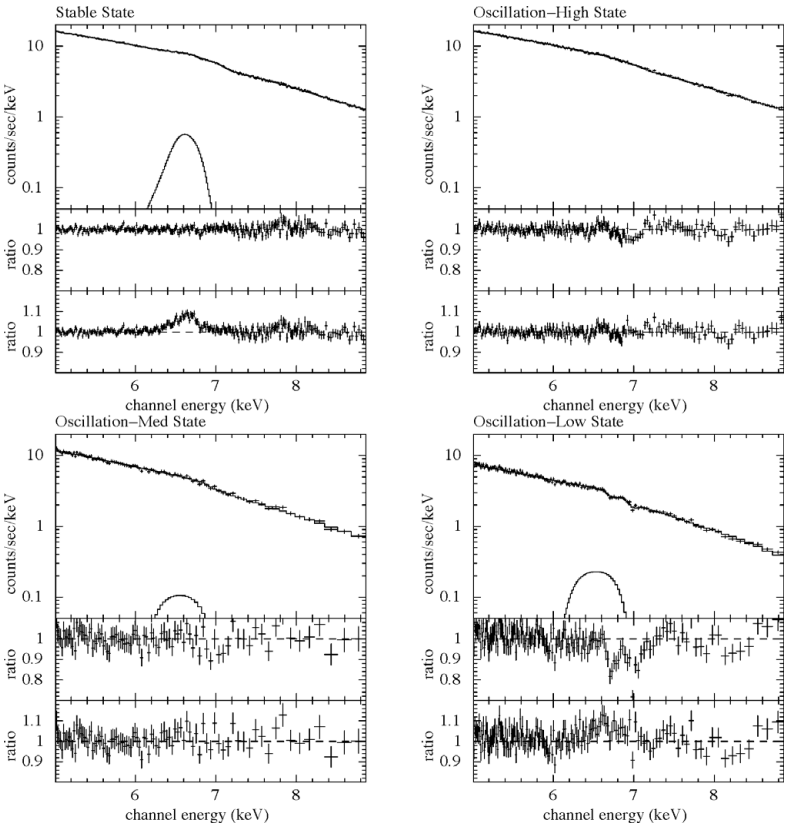

Figure 5. The XIS spectra in the 5–9 keV band. The solid curve represents the best-fit model and the contribution from the iron-K emission is separately plotted. The middle (bottom) panel plots the spectral ratio between the data and the model when the iron-K absorption (emission) lines are excluded. From left to right and top to bottom, stable, oscillation-high, oscillation-med, and oscillation-low state.

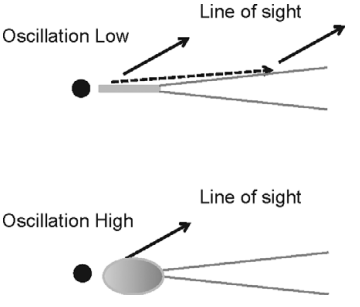

Figure 6. The schematic view of the accretion disk structure of GRS 1915+105 in the oscillation low state (dip, State A) and oscillation high state (flare, State C). The filled circle and gray area shows the black hole and inner accretion disk, respectively. During the flare phase, expansion of the inner disk causes self-shielding as viewed from the outer disk, which eliminates the iron-K emission feature, the reprocessed IR emission, and possibly the launch of the disk wind.

https://doi.org/10.1017/S1743921310016091 Published online by Cambridge University Press

References

Arai, A., *et al.* 2009, *PASJ*, 61, L1
Belloni, T., *et al.* 2000, *A&A*, 355, 271
Coppi, P. S., 1999, in "High Energy Processes in Accreting Black Holes", ASP Conference Series 161, ed. Poutanen, J., & Svensson, R. (San Francisco: Astron. Soc. Pac.), p. 375
Corbel, S., & Fender, R. P. 2002, *ApJ*, 573, L35
Corbel, S., *et al.* 2003, *A&A*, 400, 1007
Fender, R., & Belloni, T. 2004, *ARAA*, 42, 317
Gandhi, P., *et al.* 2010, *MNRAS*, 407, 2166
Makishima, K., *et al.* 1986, *ApJ*, 308, 635
Makishima, K., *et al.* 2008, *PASJ*, 60, 585
Markoff, S., *et al.* 2003, *A&A*, 397, 645
Miller, J. M., *et al.* 2006, *ApJ*, 653, 525
Miller, J. M., *et al.* 2008, *ApJ*, 679, L113
Mitsuda, K., *et al.* 1984, *PASJ*, 36, 741
Neilsen, J., & Lee, J. C. 2009, *Nature*, 458, 481
Poutanen, J., & Svensson, R. 1996, *ApJ*, 470, 249
Shidatsu, M., *et al.* 2010, *ApJ*, submitted
Tomsick, J. A., *et al.* 2009, *ApJ*, 707, L87
Ueda, Y., *et al.* 2006, in "VI Microquasar Workshop: Microquasars and Beyond", ed. T. Belloni (Como: Proc. Science), p. 23.1
Ueda, Y., Yamaoka, K., & Remillard, R. 2009, *ApJ*, 695, 888
Ueda, Y., *et al.* 2010, *ApJ*, 713, 257
Yamada, S., *et al.* 2009, *ApJ*, 707, L109

Discussion

YUAN: How precisely we know about the stable luminosity of GRS 1915? This is potentially the only super-Eddington BH. This is importan since almost all quasars are sub-Eddington.

UEDA: Typically, 30% of $L_{\rm Edd}$, but not always constant.

FALCKE: You ruled out the jet/non-thermal model from Markoff *et al.* for your Suzaku data in favor of thermal Comptonization. What is the difference in chi-squared if you compare both models?

UEDA: I din not perform fitting to our SED yet, but see a recent paper by Gandhi *et al.* (2010).

KYLAFIS: I disagree with your statement that the spectrum of 339-4 can be fitted by thermal Comptonization but not by non-thermal. On the contrary, if thermal Comptonization can fit a spectrum, non-thermal (as in a jet) can do it more easily.

UEDA: I don't agree, although fitting with a "pure" thermal Comptonization would be an extreme case and we may need to consider a non-thermal component as well.

https://doi.org/10.1017/S1743921310016091 Published online by Cambridge University Press